DOT/FAA/PM-87/18

**Project Report**
**ATC-142**

# Study of Microburst Detection Performance During 1985 in Memphis, TN

**J. T. DiStefano**

**5 August 1987**

**Lincoln Laboratory**
MASSACHUSETTS INSTITUTE OF TECHNOLOGY
*LEXINGTON, MASSACHUSETTS*

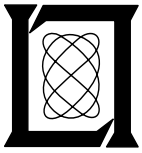

Prepared for the Federal Aviation Administration,
Washington, D.C. 20591

This document is available to the public through
the National Technical Information Service,
Springfield, VA 22161

MASSACHUSETTS INSTITUTE OF TECHNOLOGY
LINCOLN LABORATORY

# STUDY OF MICROBURST DETECTION PERFORMANCE DURING 1985 IN MEMPHIS, TN

*J.T. DiSTEFANO*
*Group 43*

PROJECT REPORT ATC-142

5 AUGUST 1987



LEXINGTON MASSACHUSETTS

## ABSTRACT

This report focuses on the detectability of microbursts using pulse Doppler weather radars and surface anemometers. The data used for this study were collected in the Memphis, TN area during the FLOWS* project of 1985. The methods used for declaring a microburst from both Doppler radar and surface anemometer data are described.

A main objective in this report was to identify the results that were generated by comparing the 1985 radar detected microbursts (which impacted the surface anemometer system) with the surface mesonet detected microbursts. In so doing, the issue of missed microburst detections, for which there occurred two (both by the radar), is identified. Possible reasons as to why these two microbursts were not detected are discussed in detail.


*FAA/Lincoln Laboratory Observational Weather Studies.

TABLE OF CONTENTS

LIST OF ILLUSTRATIONS

# LIST OF TABLES

## ACRONYMS

| | |
|---|---|
| AGL | Above Ground Level |
| FAA | Federal Aviation Administration |
| FLOWS | FAA/Lincoln Laboratory Observational Weather Studies |
| FL2 | FAA/Lincoln Laboratory Test-bed Doppler Radar |
| GMT | Greenwich Mean Time |
| LLWAS | Low-Level Windshear Alert System |
| LST | Local Standard Time |
| Mesonet | Refers to a network of automatic weather stations with a close, i.e., a "mesoscale" spacing. |
| MSL | Mean Sea Level |
| PPI | Plan Position Indicator |
| PROBE | Portable Remote OBservations of the Environment |
| UND | University of North Dakota |

# I. INTRODUCTION

In 1985, Memphis, TN was the site for the FAA/Lincoln Laboratory Observational Weather Studies (FLOWS) program [Evans and Johnson, 1984]. During this time, radar and surface anemometer data were collected on low-level wind shear events that could be potential hazards to aviation. Investigations are on-going as to the detectability and predictability of wind shear events, in particular gust fronts and microbursts. This report will focus on the detectability of microbursts using pulse Doppler weather radars and surface anemometers.

Data on these microbursts were collected simultaneously with both radar and surface mesonet sensors. The radars used were an S-band radar (FL2) developed and operated by Lincoln Laboratory for the FAA [Evans and Turnbull, 1985] and a C-band radar that was operated by the University of North Dakota (UND). The FL2 and UND radars were located approximately 10 km south and 15 km southeast of the Memphis International Airport, respectively (see Figure I-1). The surface mesonet consisted of 30 PROBE (Portable Remote OBservations of the Environment) weather stations [Wolfson, et al., 1986] and 6 Low-Level Windshear Alert System (LLWAS) sensors. The PROBE stations collected data on several meteorological parameters (barometric pressure, relative humidity, temperature, precipitation rates, average and peak wind speed and direction) while the LLWAS sensors just recorded wind speed and direction. The locations of these 36 sensors are also shown in Figure I-1. The horizontal and vertical lines in this figure represent the runways of the Memphis International Airport (located approximately 10 km north of the UND radar).

The primary objective of this performance evaluation was to compare the 1985 radar detected microbursts, which were observed over (or in the close proximity to) the surface mesonet, with the mesonet detected microbursts. In comparing these two data sets, the issue of missed detections, either by the mesonet or radar, was addressed. For the events that were categorized as possible missed detections by the radar based on expert human analysis of the radar data fields, the microburst outflow detection algorithm developed by Merritt (1987) was used on the radar data and the results noted.

The second chapter describes the methodology used for declaring microbursts when analyzing radar or surface mesonet data. Chapter III discusses the overall results of the radar/mesonet comparison of microburst detections and chapter IV details the two particular cases that fell into the category of "missed detections" by the radar. Chapter V briefly summarizes the conclusions while the last chapter identifies some plans for future analysis of the 1985 data.

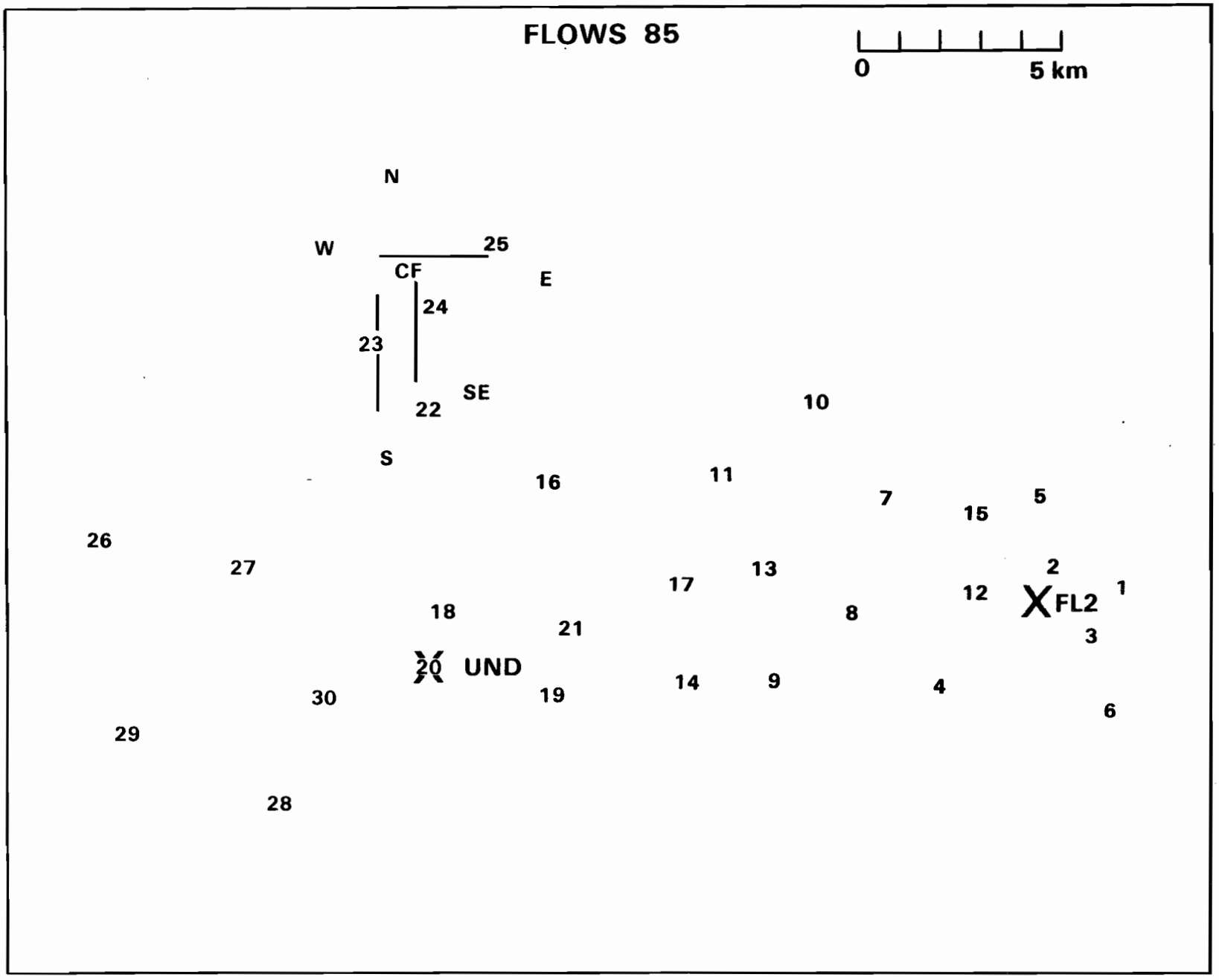


Figure I-1. The FLOWS 1985 mesonet at Memphis, TN (2 radars, 30 mesonet PROBE stations, and 6 LLWAS stations).

## II. METHODOLOGY USED IN DECLARING A MICROBURST

Fujita describes a downburst as a strong downdraft which induces a microburst of damaging* winds on or near the ground. The outburst winds, either straight or curved, are highly divergent [Fujita, 1985]. He subdivides the downburst into two categories depending on the outbursts' horizontal scale:

1) macroburst - a large downburst with its' outburst winds extending in excess of 4 km in the horizontal direction, and

2) microburst - a small downburst with its' outburst extending only 4 km or less in the horizontal.

This divergent outburst, which was the main microburst identifying feature, was searched for in both the FL2 and surface mesonet data sets.

### A. Using Doppler Radar Data

In both real time and playback modes, the microburst signature was identified in the Doppler velocity field by a divergent outflow at or near the surface. The observed minimum differential velocity values within this outflow had to reach 10 m/s within a range extent of 4 km and maintain this magnitude for at least two successive scans in order for a microburst to be declared. These threshold values are also used in the microburst detection algorithm [Merritt, 1987]. Figure II-1 portrays an ideal surface divergent signature produced by a microburst outflow. The radar in this figure observes a radial velocity couplet, where the negative values are velocities approaching the radar while positive values are receding. Realistically, however, not all microbursts demonstrate this clear signature.

### B. Using Surface Mesonet Data

Once the surface mesonet data have been received at Lincoln Laboratory and converted to a common format, they are inventoried and plotted for immediate analysis. From this initial look at the data and from the FLOWS operational field logs, the days and times on which microbursts (and other wind shear events) may have occurred over the mesonet are determined [Wolfson, et al, 1986]. A primary indicator of the microburst, through this initial analysis, is given by the profile of the wind speed where an isolated peak may be identified. Other parameters (along with wind speed) such as wind direction, barometric pressure, temperature, precipitation rate, and relative humidity may also aid in the declaration process for a microburst. Statistics on these identifying parameters are discussed by Fujita (1985) and Rinehart, et al. (1986).

*It should be noted that the wind shear which accompanies these events may be hazardous to aviation but may not necessarily produce damage to impacted structures or landscape.

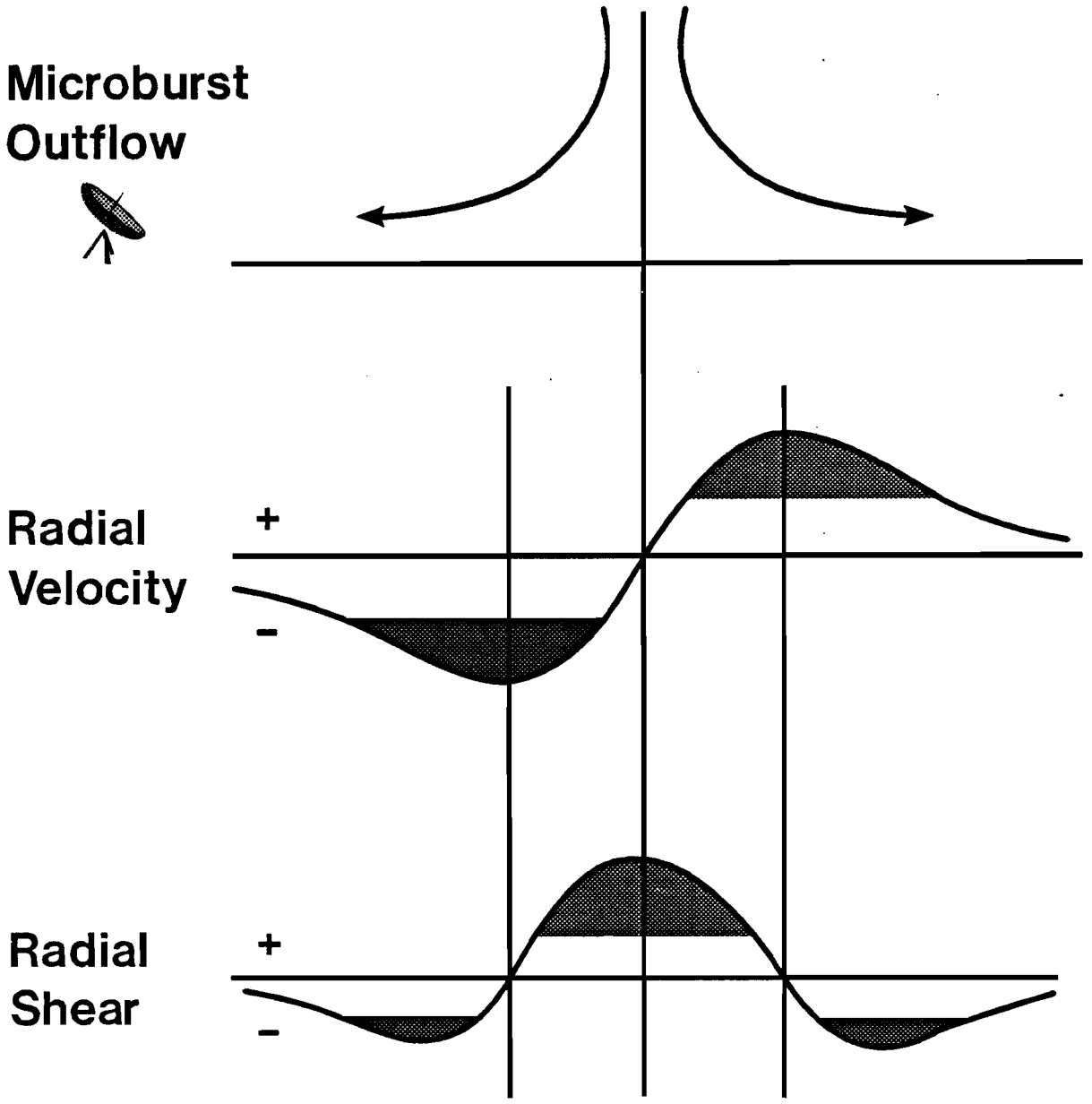


Figure II-1. Microburst surface divergence signatures.

Several steps, involving both objective and subjective analysis, are then taken to confirm and classify the event(s) [Wolfson, et al., 1986]. Probably the most important part of this analysis is identifying the surface divergence over the mesonet. Once this surface signature, such as seen in Figure II-2, is identified, the strength of the event as observed by the differential velocity is calculated. In order for the event to be classified as a microburst, it must attain a differential velocity value of 10 m/s within a distance of 4 km. This is the same threshold value used in identifying a microburst from the analysis of Doppler velocity fields.

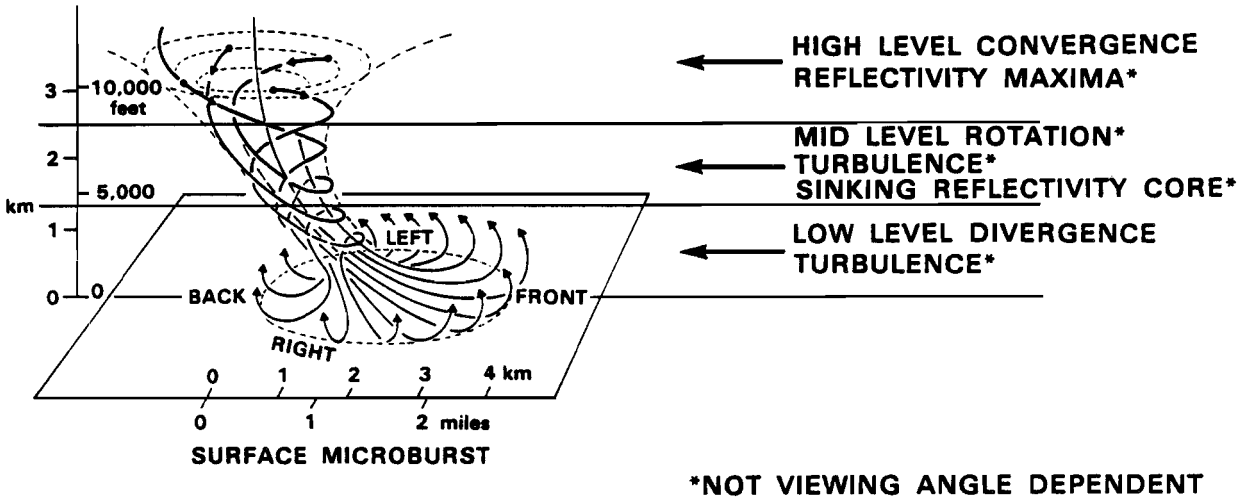


Figure II-2. Generalized model of a microburst.

## III. OVERALL RESULTS

During the 1985 data collection season, it was estimated based on Doppler radar and mesonet data that 45 microbursts impacted the FLOWS mesonet. It is possible that there may have been more events since not all of the radar data collected had been exhaustively examined. Also, some events may have gone undetected by the radar due to site obstructions in which an average of ≈1° blockage above the horizon was noted. Also, during periods of the project when the aircraft flew [Rinehart, et al., 1986], the site did not always observe the velocity field at the surface. Figure III-1 shows the approximate locations, with respect to the FL2 mesonet, of the 45 known events. Of these, 3 were without accompanying data from either the FL2 or UND radars (see Table III-1). Therefore, relevant to this study were the 42 microbursts that were observed by the surface mesonet sensors and the radar(s).

After the data sets for these 42 cases had been compared, it was observed that ≈95.2% (40 of 42 cases) were detected by both the mesonet and the radar. This left 2 cases, or 4.8%, for which the mesonet clearly identified a microburst, but the radar data did not.

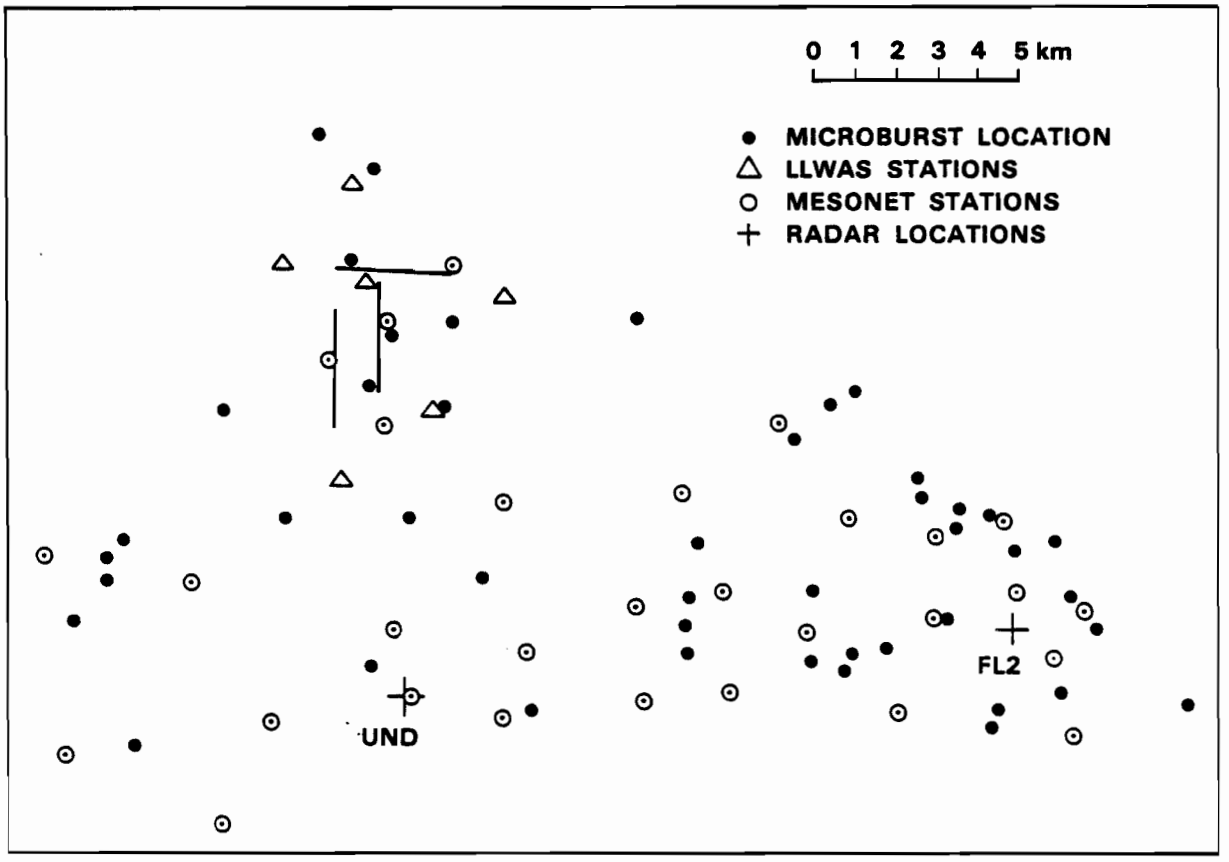


Figure III-1. Locations of the 1985 mesonet impacting microbursts.

Table III-1(a)

1985 Mesonet Impacting Microbursts

Maximum velocity differentials observed by the radar(s) for each event are given. The third column, labeled "Time (GMT)" refers to the time at which the microburst was observed by the surface mesonet. The last column, labeled "Time Observed by Radar" refers to the time at which the maximum ΔV was observed by the radar. (Y=Yes, N=No, ND=No Data, NA=Not Applicable)

| MB# | Date | Time (GMT) | Detected by: MESO | FL2 | UND | Approx. Max ΔV (m/s) | Approx. Couplet Values (m/s) | Time Observed by Radar (GMT) |
|---|---|---|---|---|---|---|---|---|
| 1 | 24 MAR | 0135-0200 | Y | ND | ND | -- | ------ | ---- |
| 2 | 31 MAR | 0303-0322 | Y | Y | NA | 17 | -10,+7 | 0316 |
| 3 | 23 APR | 2023-2044 | Y | Y | | 13 | -5,+8 | 2021 |
| | | | | | Y | 12 | -5,+7 | 2023 |
| 4 | 24 APR | 2359-0012 | Y | N | N | --- | ----- | ---- |
| 5 | 30 APR | 2140-2155 | Y | Y | | 17 | -5,+12 | 2144 |
| | | | | | Y | 31 | -6,+25 | 2144 |
| 6 | 30 APR | 2200-2224 | Y | Y | NA | 27 | -12,+15 | 2209 |
| 7 | 7 MAY | 1822-1845 | Y | ND | Y | 22 | -14,+8 | 1832 |
| 8 | 11 MAY | 2050-2105 | Y | ND | ND | --- | ----- | ---- |
| 9 | 14 MAY | 2125-2150 | Y | Y | NA | 15 | -10,+5 | 2134 |
| 10 | 18 JUN | 0001-0010 | Y | Y | | 14 | -7,+7 | 0008 |
| | | | | | Y | 15 | -10,+5 | 0005 |
| 11 | 25 JUN | 1815-1830 | Y | Y | NA | 10 | -4.5,+5.5 | 1819,-21,-23 |
| 12 | 25 JUN | 2302-2330 | Y | Y | NA | 25 | -10,+15 | 2329 |
| 13 | 26 JUN | 1900-1930 | Y | Y | NA | 30-36+ | -18,+12-28 | 1858-1900 |
| 14 | 26 JUN | 1931-2000 | Y | Y | NA | 27 | -15,+12 | 1945 |
| 15 | 27 JUN | 2155-2210 | Y | Y | NA | 22 | -7,+15 | 2159 |
| 16 | 27 JUN | 2205-2210 | Y | Y | NA | 25 | -7,+18 | 2205 |
| 17 | 30 JUN | 2246-2315 | Y | Y | NA | 26 | -10,+16 | 2304 |
| 18 | 11 JUL | 0025-0035 | Y | Y | NA | 30 | -12,+18 | 0029 |
| 19 | 15 JUL | 1944-1955 | Y | Y | NA | 16 | -9,+7 | 1947 |
| 20 | 15 JUL | 2006-2011 | Y | Y | | 18 | -10,+8 | 2006 |
| | | | | | Y | 18 | -10,+8 | 2010 |
| 21 | 15 JUL | 2015-2040 | Y | Y | NA | 24 | -12,+12 | 2019 |
| 22 | 15 JUL | 2115-2132 | Y | ND | Y | 16 | -7,+9 | 2117 |
| 23 | 15 JUL | 2135-2143 | Y | ND | Y | 10 | -5,+5 | 2139 |
| 24 | 23 JUL | 1800-1813 | Y | Y | NA | 18 | -7,+11 | 1801 |
| 25 | 23 JUL | 2033-2039 | Y | N | ND | --- | ------ | ---- |
| 26 | 9 AUG | 2048-2055 | Y | Y | NA | 12 | -4,+8 | 2053 |
| 27 | 10 AUG | 2009-2014 | Y | Y | | 17 | -5,+12 | 2010 |
| | | | | | Y | 16 | -10,+6 | 2011 |
| 28 | 11 AUG | 2329-2350 | Y | ND | ND | --- | ------ | ---- |
| 29 | 15 AUG | 2038-2055 | Y | Y | NA | 20 | -15,+5 | 2038 |
| 30 | 15 AUG | 2106-2119 | Y | Y | NA | 18 | -10,+8 | 2109 |
| 31 | 15 AUG | 2108-2126 | Y | Y | NA | 23 | -7,+16 | 2119 |
| 32 | 24 AUG | 1523-1527 | Y | Y | NA | 13 | -8,+5 | 1525 |
| 33 | 24 AUG | 1528-1546 | Y | Y | | 17 | -12,+5 | 1530 |
| | | | | | Y | 20 | -8,+12 | 1530 |

Table III-1(a). (Continued)

| MB# | Date | Time (GMT) | Detected by: MESO | FL2 | UND | Approx. Max ΔV (m/s) | Approx. Couplet Values (m/s) | Time Observed by Radar (GMT) |
|---|---|---|---|---|---|---|---|---|
| 34 | 24 AUG | 2011-2030 | Y | Y | NA | 17 | -12,+5 | 2013 |
| 35 | 25 AUG | 0730-0800 | Y | ND | Y | 25 | -13,+12 | 0738 |
| 36 | 7 SEP | 2028-2040 | Y | Y | NA | 11 | -5,+6 | 2044* |
| 37 | 7 SEP | 2110-2140 | Y | Y | NA | 20 | -10,+10 | 2118,-20 |
| 38 | 7 SEP | 2212-2226 | Y | Y | NA | 16 | -8,+8 | 2219 |
| 39 | 7 SEP | 2302-2323 | Y | Y | NA | 16 | -10,+6 | 2307 |
| 40 | 8 SEP | 1809-1900 | Y | Y | NA | 12 | -7,+5 | 1821 |
| 41 | 8 SEP | 1835-1847 | Y | Y | NA | 22 | -15,+7 | 1838 |
| 42 | 8 SEP | 1852-1900 | Y | Y | NA | 15 | -7,+8 | 1853 |
| 43 | 8 SEP | 1854-1901 | Y | Y | NA | 22 | -15,+7 | 1853 |
| 44 | 8 SEP | 1914-1920+ | Y | Y | NA | 14 | -7,+7 | 1920 |
| 45 | 8 SEP | 1918-1930 | Y | Y | | 13 | -16,-3 | 1925 |
| | | | | | Y | 20 | -8,+12 | 1924 |

*no radar data prior to this time.

Table III-1(b)

Locations of the 1985 Mesonet Impacting Microbursts

A list of the approximate locations (relative to the FL2 and UND radar sites) for each 1985 mesonet impacting microburst.

| | | FL2 | | UND | |
|---|---|---|---|---|---|
| MB# | Date | Range (km) | Azimuth (°) | Range (km) | Azimuth (°) |
| 1 | 24 MAR | 20 | 285 | 9 | 320 |
| 2 | 31 MAR | 13 | 275 | 3 | 030 |
| 3 | 23 APR | 1.25 | 060 | 16 | 082 |
| 4 | 24 APR | 5 | 280 | 10 | 075 |
| 5 | 30 APR | 17 | 290 | 7.5 | 355 |
| 6 | 30 APR | 3-4 | 250-325 | 12-13 | 087-067 |
| 7 | 7 MAY | 22 | 275 | 7.5 | 295 |
| 8 | 11 MAY | 4 | 250 | 11 | 088 |
| 9 | 14 MAY | 3 | 260 | 12 | 085 |
| 10 | 18 JUN | 22.5 | 273 | 7.5 | 295 |
| 11 | 25 JUN | 18 | 298 | 10 | 355 |
| 12 | 25 JUN | 15 | 280 | 4 | 000 |
| 13 | 26 JUN | 7 | 325 | 13 | 055 |
| 14 | 26 JUN | 16 | 298 | 8 | 005 |
| 15 | 27 JUN | 2 | 195 | 14 | 090 |
| 16 | 27 JUN | 4-7 | 105-125 | 18-21 | 088-106 |
| 17 | 30 JUN | 22 | 262 | 6 | 260 |
| 18 | 11 JUL | 2 | 140 | 16 | 090 |
| 19 | 15 JUL | 2 | 026 | 16 | 075 |
| 20 | 15 JUL | 3 | 335 | 19 | 070 |
| 21 | 15 JUL | 4 | 328 | 13 | 065 |
| 22 | 15 JUL | 2.5 | 348 | 19 | 073 |
| 23 | 15 JUL | 3 | 330 | 18 | 072 |
| 24 | 23 JUL | 7 | 320 | 12.5 | 056 |
| 25 | 23 JUL | 22.5 | 272 | 7.5 | 295 |
| 26 | 9 AUG | 21 | 305 | 13 | 350 |
| 27 | 10 AUG | 2.5 | 195 | 14 | 091 |
| 28 | 11 AUG | 23 | 270 | 8.5 | 282 |
| 29 | 15 AUG | 2 | 090 | 16 | 085 |
| 30 | 15 AUG | 12 | 260 | 3 | 090 |
| 31 | 15 AUG | 7 | 310 | 12 | 060 |
| 32 | 24 AUG | 2 | 000 | 15 | 075 |
| 33 | 24 AUG | 4 | 260 | 12 | 085 |
| 34 | 24 AUG | 18 | 278 | 6 | 320 |
| 35 | 25 AUG | 15 | 290 | 7 | 005 |
| 36 | 7 SEP | 8 | 285 | 8 | 060 |
| 37 | 7 SEP | 8 | 275 | 7 | 070 |
| 38 | 7 SEP | 8 | 265 | 7 | 080 |
| 39 | 7 SEP | 5 | 260 | 10 | 082 |
| 40 | 8 SEP | 2 | 277 | 13 | 081 |
| 41 | 8 SEP | 12 | 309 | 11 | 034 |
| 42 | 8 SEP | 8 | 270 | 7 | 075 |
| 43 | 8 SEP | 19 | 305 | 13 | 354 |
| 44 | 8 SEP | 16 | 266 | 1 | 315 |
| 45 | 8 SEP | 17 | 295 | 9 | 356 |

## IV. DETAILS OF CASES WHERE RADAR DID NOT DETECT THE MICROBURST

### A. Case 1: 23-24 April 1985

The surface mesonet plots, for this case, depict a microburst outflow signature centered in the vicinity of station #8, which is approximately 5 km west of the FL2 radar site (Figure IV-1). Maximum divergence and differential velocity ($\Delta V$), which was computed using the actual measured winds over the mesonet, are shown for this event in Figure IV-2(a). Threshold values of $2.5 \times 10^{-3} s^{-1}$ and 10 m/s were exceeded for both divergence and $\Delta V$, respectively (especially between 2355 and 0005 (GMT)). Looking at only the radial component of the mesonet surface winds (with respect to the FL2 radar site), it is shown that maximum divergence values peak at greater than $5 \times 10^{-3} s^{-1}$ while maximum $\Delta V$'s predominantly fall under the threshold value of 10 m/s (see Figure IV-3(a)). When comparing these values with those taken from the actual wind measurements, the major differences are seen in the $\Delta V$ plots. Two possible factors contributed to this inconsistency:

1) The mesonet surface sensors seemed to indicate the asymmetric nature of this event (see Figure IV-1). The strongest winds were east of the microburst center with very little back-flow evident. This could be attributed to the environmental winds being rather strong from the west-southwest and coupled with the fact that a gust front had just crossed the eastern portion of the network. The microburst was situated, relative to the high winds associated with the gust front, such that there appeared to be one asymmetric wind shear event.

2) This event seemed to encompass the FL2 radar site. For this case, the radial component of the mesonet winds, with respect to FL2, were examined in order to relate to that which was observed by the radar. In doing this, a problem with identifying the magnitude (and even the existence) of this microburst was encountered (as shown by the contrasting differential velocity plots in Figures IV-2(a) and IV-3(a)). This occurred because the microburst was impacting the radar and therefore its signature could not be completely observed along a radial. Human analysts, as well as the current microburst detection algorithm, typically have trouble identifying microbursts that impact the radar for precisely this reason.

FL2 resampled radar data shows, for this case, reflectivity values of 45+ dBz within 5+ kilometers of the radar. This strong reflectivity encompasses the eastern third of the mesonet. Divergence and $\Delta V$ values seen at 0.5° and 1.5°elevation angles would appear to be weak. Figure IV-4 shows an FL2 reflectivity and Doppler velocity field at ≈0000 (GMT) [1800 LST]. This resampled data was then compared with the raw radar data. This was done to see if any relevant data had been smoothed and/or eliminated due to the averaging which occurs when the raw radial data is resampled onto the Cartesian grid. The high reflectivity levels seen in the Cartesian image agreed well with the radial reflectivity levels. In the raw Doppler velocity field, a weak area of positive (receding) values were evident at 0.5° elevation angle (Figure IV-5) which had lower values in the resampled

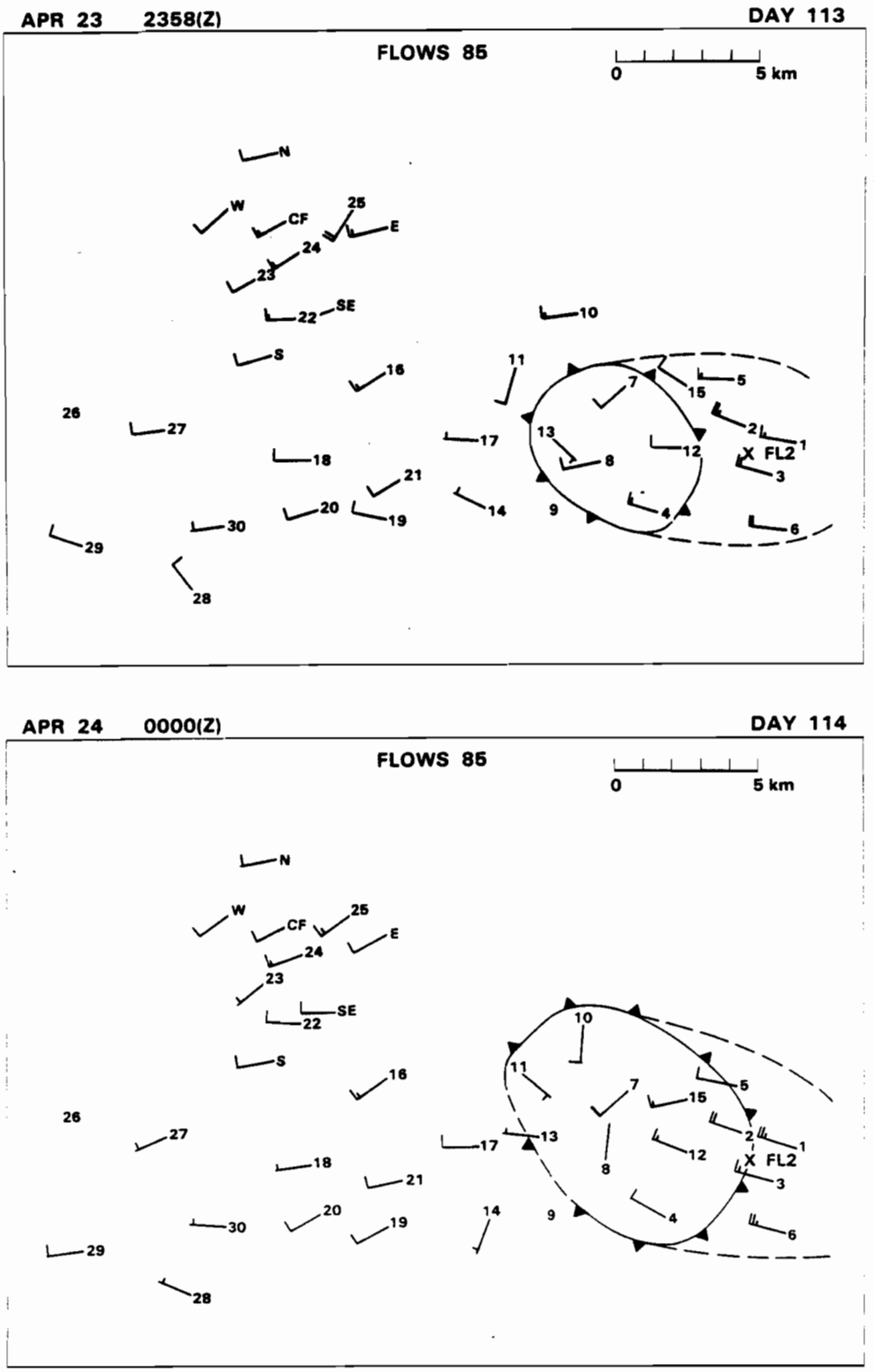


Figure IV-1. Mesonet plots showing the surface wind field for April 23, 1985 at 2358 (GMT) and April 24, 1985 at 0000 (GMT). Full barb represents 5 m/s and half-barb 2.5 m/s.

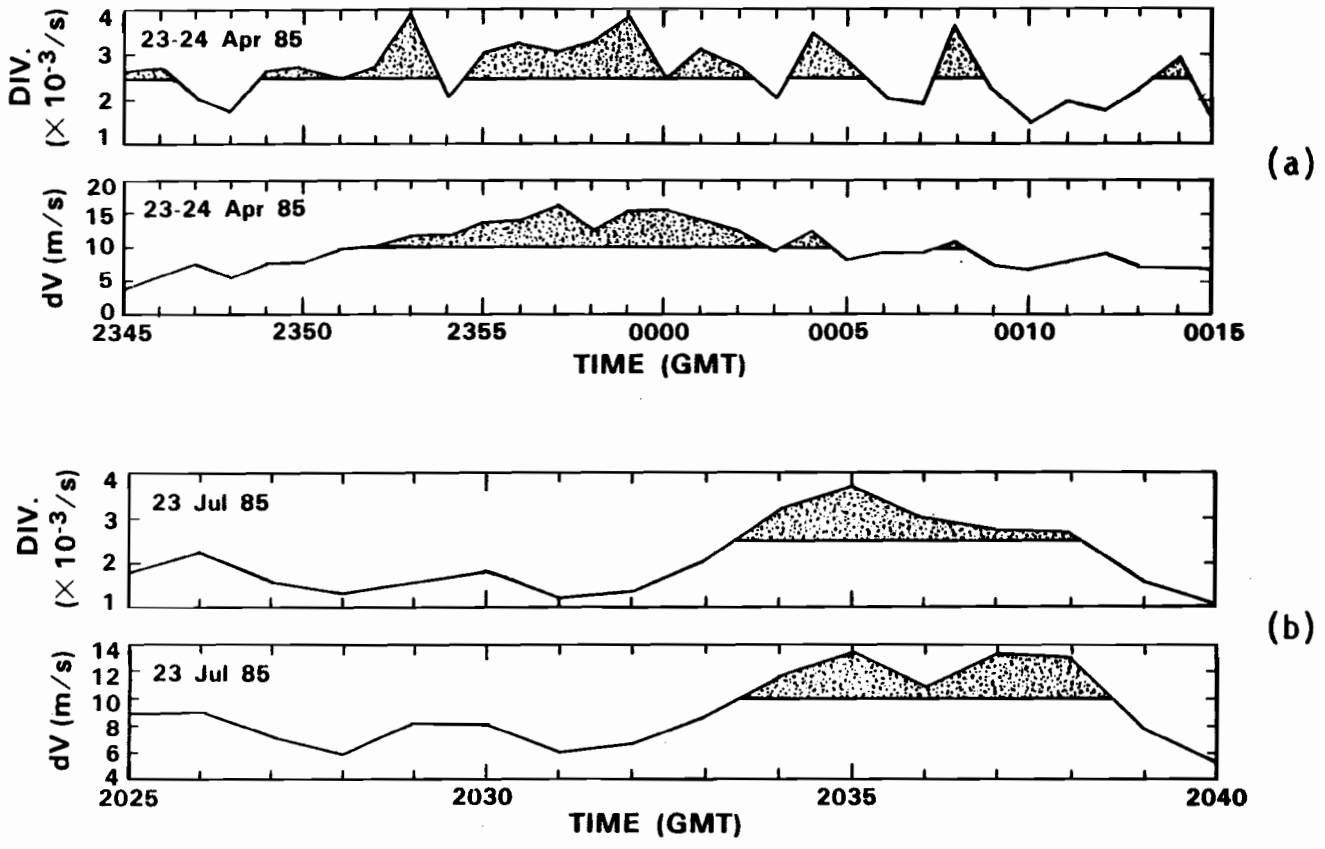


Figure IV-2. Maximum divergence and differential velocity values that were computed over the mesonet using the actual measured winds for specified times during (a) 23-24 April 1985, and (b) 23 July 1985.

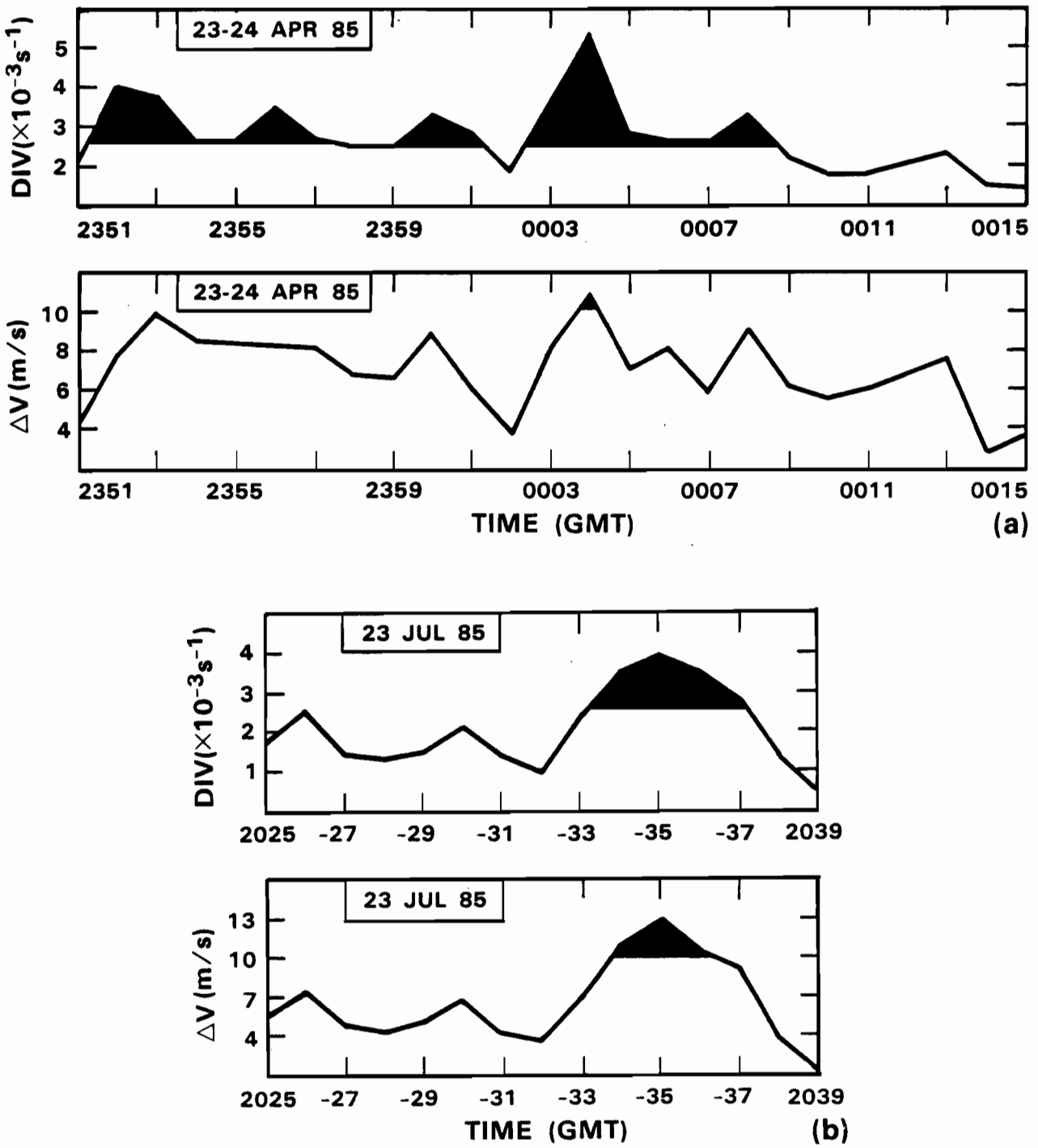


Figure IV-3. Maximum divergence and differential velocity values that were computed over the mesonet using the radial wind measurements (w.r.t. the FL2 radar site) for specified times during (a) 23-24 April 1985, and (b) 23 July 1985.

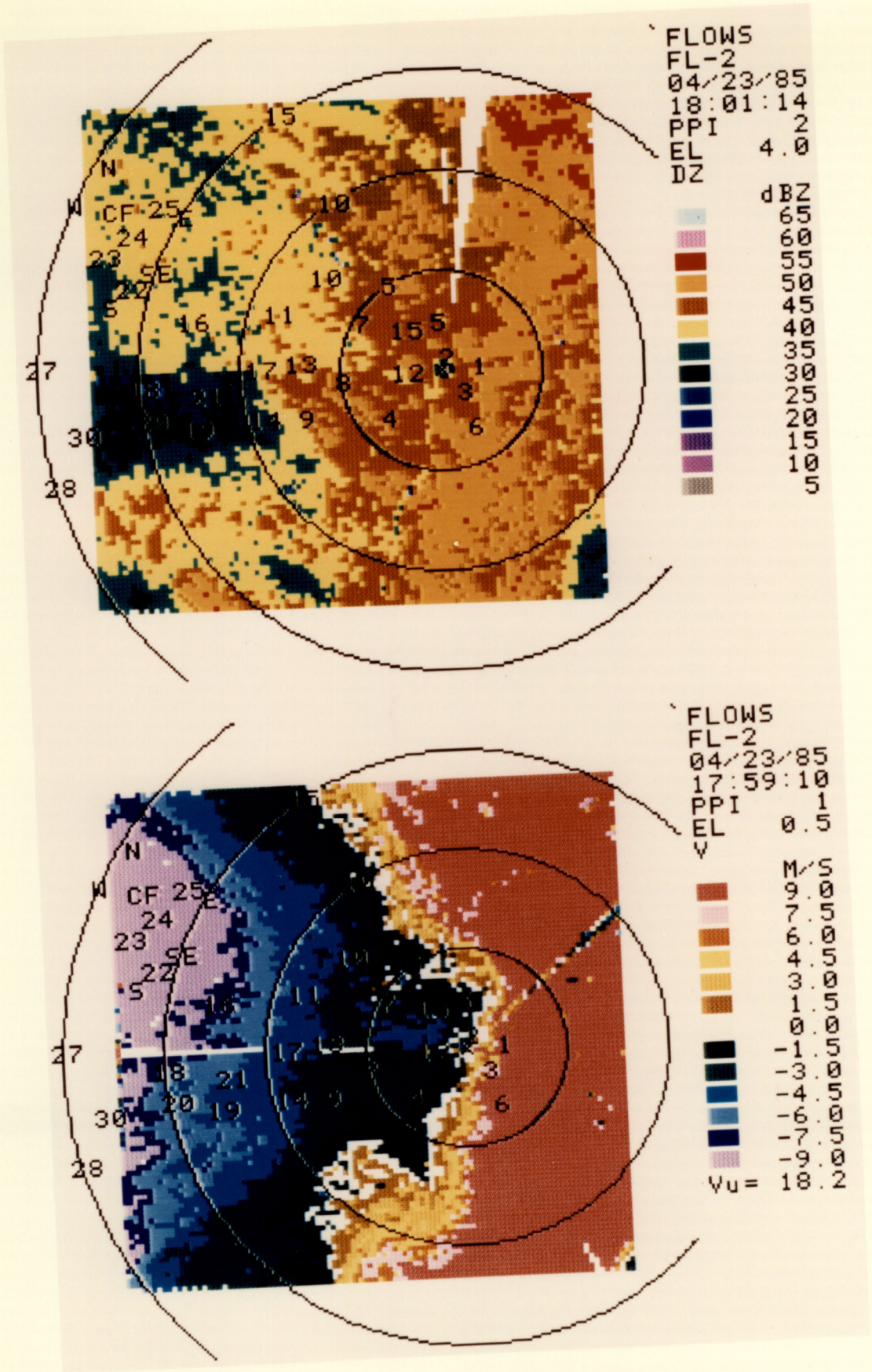


Figure IV-4. FL2 reflectivity and Doppler velocity fields for 23 April 1985 at ≈1800 LST (or ≈0000 GMT on 24 April 1985). Elevation angles for the reflectivity and velocity plots are 4° and 0.5°, respectively. Range rings are every 5 km and locations of mesonet stations are overlaid.

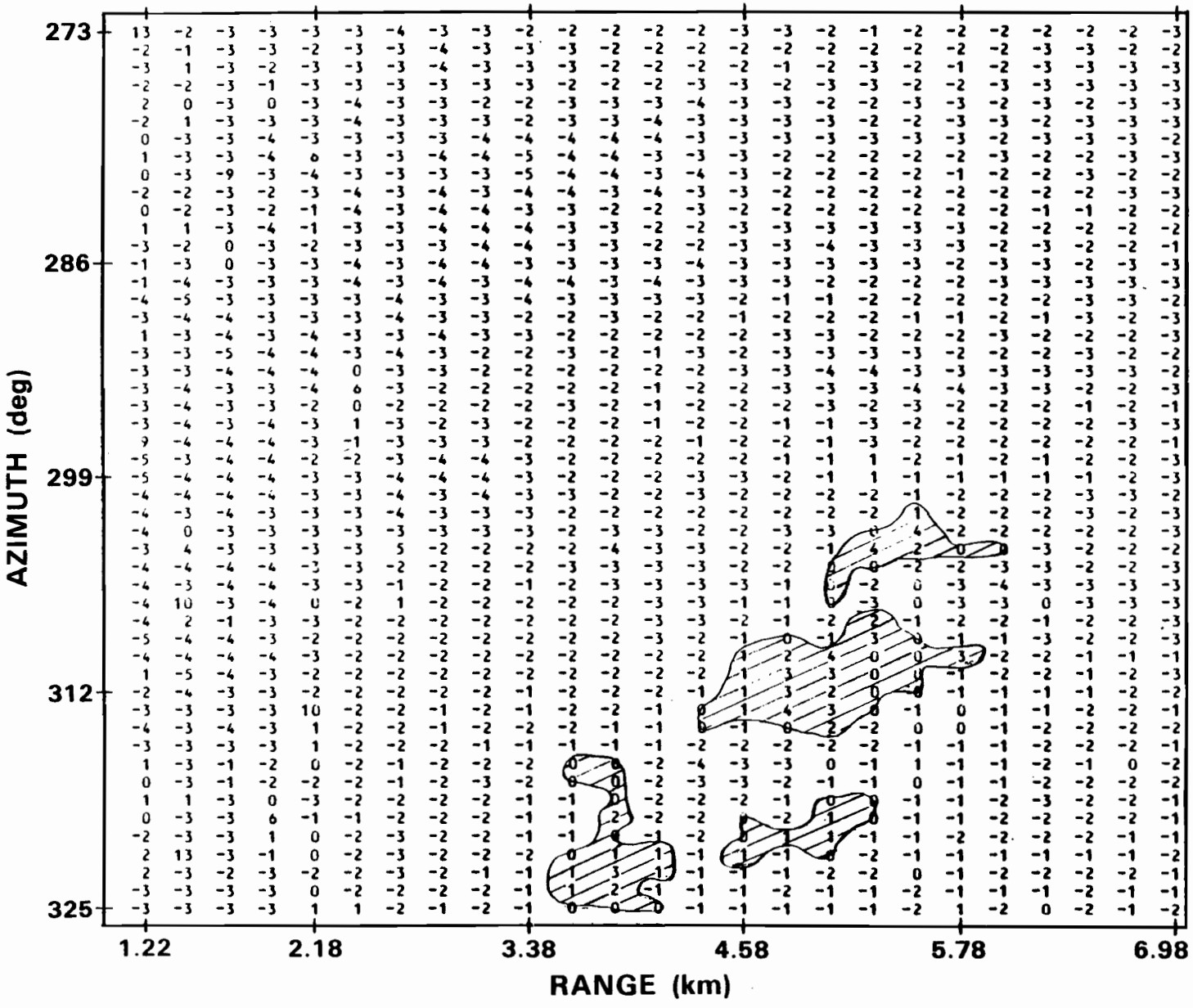


Figure IV-5. Doppler radial velocities in m/s as seen by FL2 on 23 April 1985 at ≈1759 LST (or 2359 GMT). Range and azimuthal intervals are 1.22-6.98 km and 273-325°, respectively. Elevation angle is 0.5°.

field. Nevertheless, maximum values of dV did not appear to exceed 9-10 m/s within a radial distance of ≈7 km (this distance represents the extent of a large area of divergence located just west of FL2). It should be noted that the UND radar surface scan velocity data showed no sign of a microburst event for this time period.

After analyzing the mesonet and radar data for this case, the microburst outflow detection algorithm [Merritt, 1987] was run. Its' output showed the detection of a shear region near where the mesonet identified the event, but the algorithm did not identify this as a microburst event because the shear region lacked continuity in time. As mentioned earlier, the current algorithm typically has trouble identifying a microburst which directly impacts the radar as appears to be the case here.

B. Case 2: 23 July 1985

The mesonet plots depicting the surface wind field for this date show a directionally divergent wind shear event over the extreme western portion of the network (see Figure IV-6). This event, located approximately 23 km west of FL2, mainly affected stations #26, #27, and #29. The maximum divergence and $\Delta V$ signatures, taken from the actual wind measurements for this event, are shown in Figure IV-2(b). Threshold values are exceeded for approximately 5 continuous minutes. Similar traces for these values are seen in Figure IV-3(b) where the radial component of the wind, relative to the FL2 site, is used. Again, the threshold values are exceeded but with the slight difference being in duration.

The FL2 resampled radar data for this case showed 3 separate convective cells. The one of concern was located near station #26. This cell exhibited reflectivity values greater than 55 dBz which was verified through analysis of the raw radar data. Radial velocities were weak in the area of this cell ($\leq$ 7 m/s). Likewise, maximum divergence and dV values, as viewed by the radar, would appear also to be weak. Figure IV-7 shows the FL2 reflectivity and Doppler velocity fields for 2037 (GMT) [1437 LST]. The apparent absence of any significant shear was reflected in the output from the microburst detection algorithm which identified no shear regions in the vicinity of the above mentioned event. During this case, no UND radar data were available.

There were two possible causes addressed here for as to why this event was not identified as a microburst by the FL2 radar. They are:

1) blockage of the radar beam, and/or

2) shallowness of the depth of the outflow.

Figure IV-8 shows the topography of the terrain between the FL2 radar and the wind shear event which was located approximately 23 km to the west (along the 272° azimuth line). The event, as seen by the surface network, was located in a valley at an elevation of ≈80 m (260 ft.) MSL which was ≈49 m (160 ft.) below the position of the radar. The beamwidth for the FL2

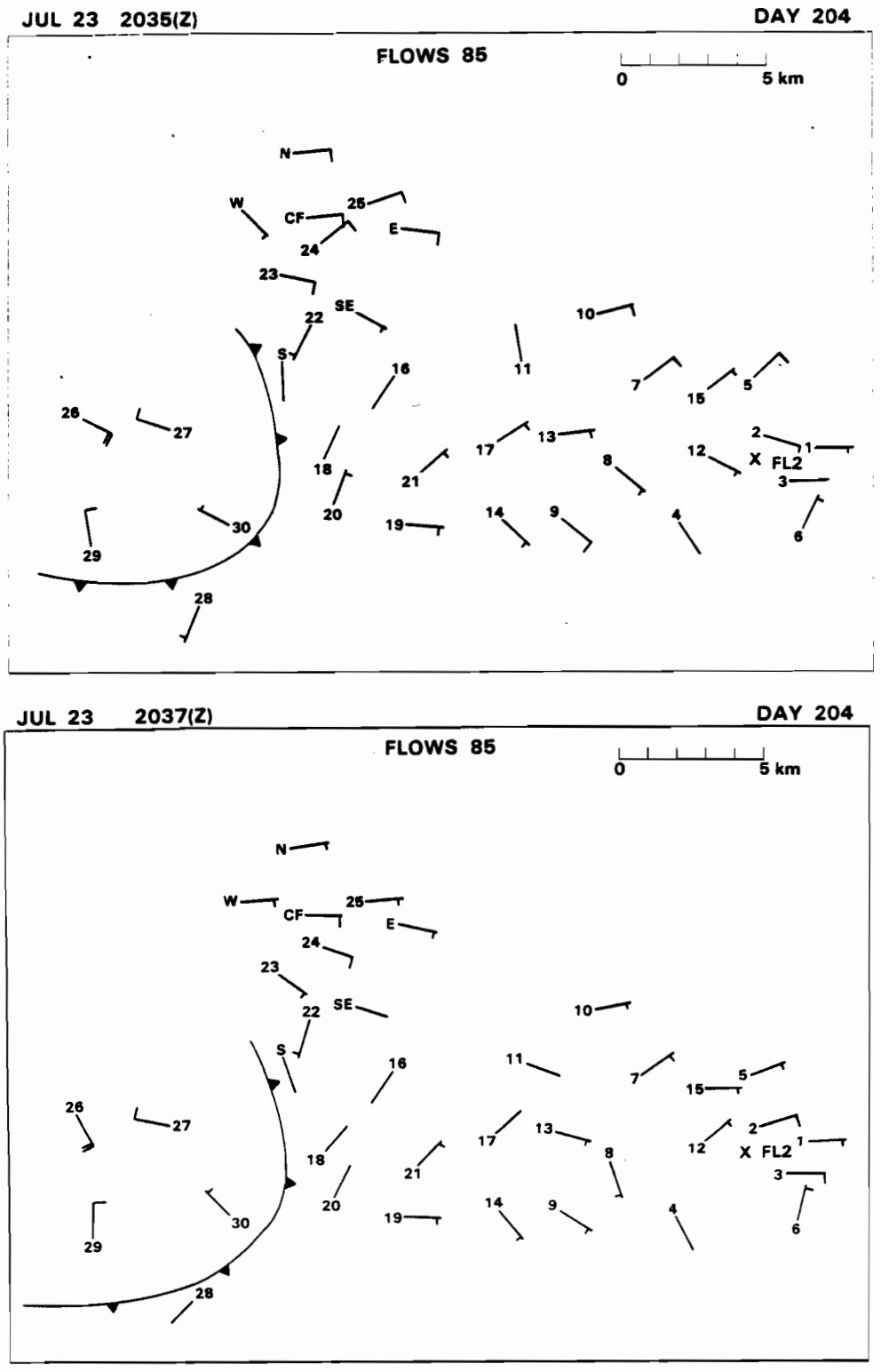


Figure IV-6. Mesonet plots showing the surface wind field for July 23, 1985 at 2035 and 2037 GMT. Full barb represents 5 m/s and half-barb 2.5 m/s.

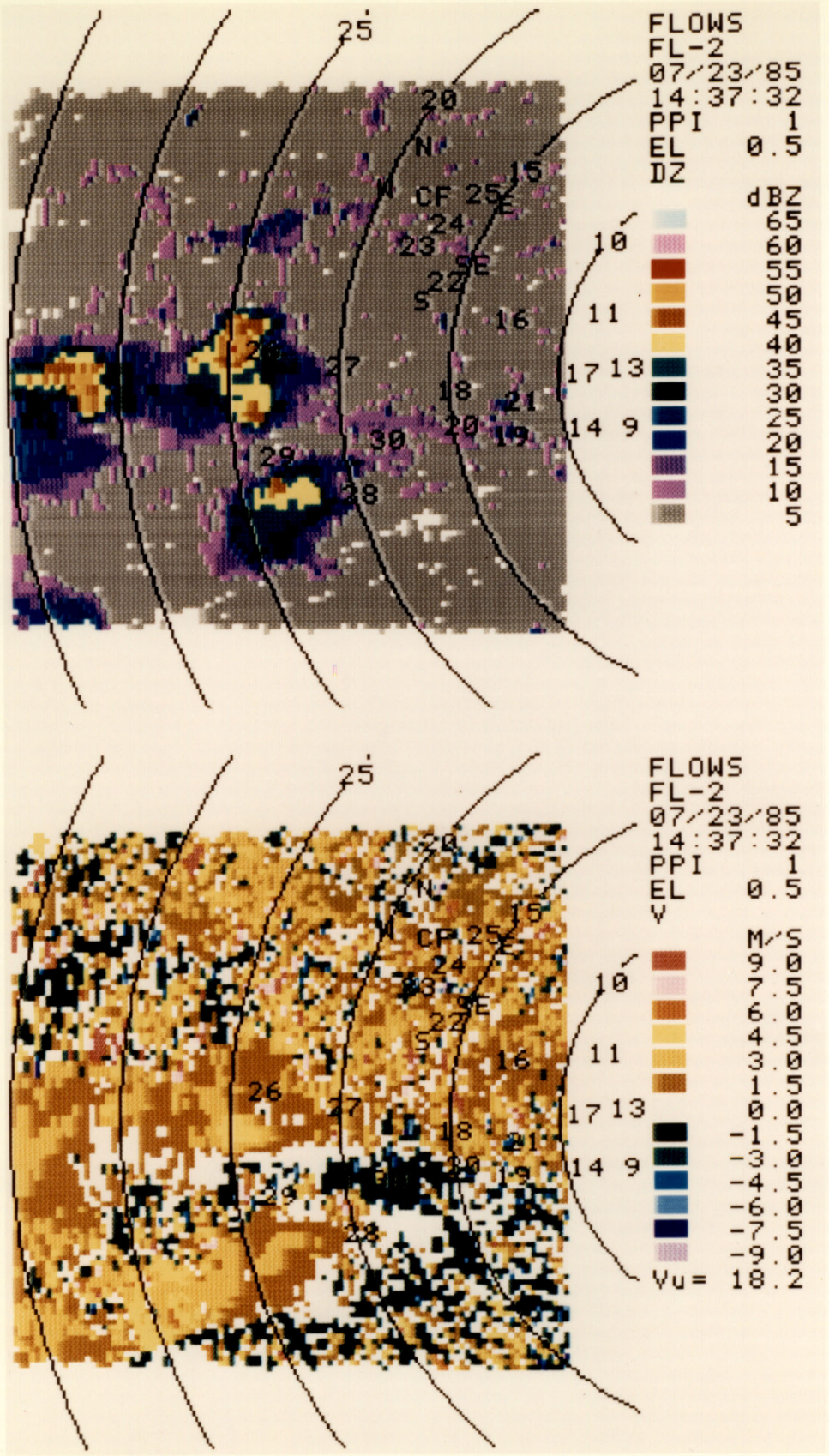


Figure IV-7. FL2 reflectivity and Doppler velocity fields for 23 July 1985 at ≈1437 GMT (or ≈2037 GMT). Elevation angle for both plots is 0.5°. Range rings are every 5 km and locations of mesonet stations are overlaid.

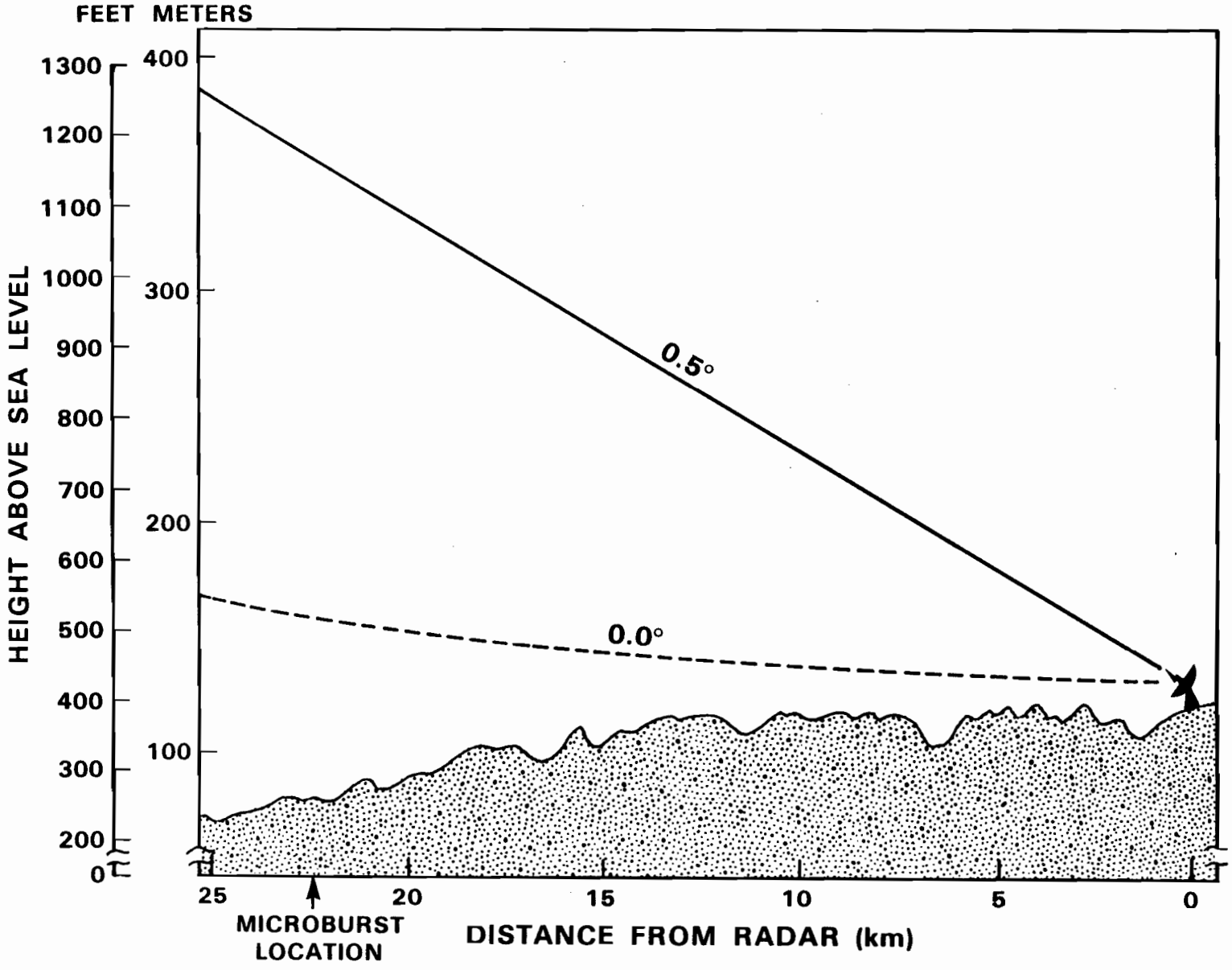


Figure IV-8. Vertical profile of the topography between the FL2 radar and points west along the 272° azimuth. With the radar at 0.5° elevation angle, the bounds of the bottom half of the beam, assuming no blockage by trees, are noted.

radar is approximately 1° [Rinehart, et al., 1986] and for this event the lowest tilt scanned was set at an elevation angle of 0.5°. This figure also depicts the boundary of the bottom half of the beam (0.0-0.5° elevation angle). The height AGL of the lower portion of the beam was ≈81 m (262 ft.) at the apparent range of the event. This figure does not indicate the presence of any orographic obstacles that might induce blockage of the beam. However, from a panoramic photograph that was taken by T. Fujita, there appears to be a line of trees a few kilometers from the radar which may obstruct a portion of the beam at this azimuth. If the trees at a range of 3 km were 80 feet high, the line of sight would have been obstructed below a height of 1100 feet above sea level (=250 m above ground level). To check this, a sequence of PPI (Plan Position Indicator) reflectivity plots were analyzed at each available tilt. If:

(1) the microburst reflectivity were constant with height over the lowest few kilometers, and

(2) blockage occurs only on the lowest beam

then one can estimate the degree of blockage by comparing the microburst reflectivity at the lowest tilt with that at upper angles. For the case at hand where the lowest beam is at most 50% blocked, the reflectivity difference would be $\leq$ 3 dB. Unfortunately, the differences between reflectivity levels for the upper tilts (where no blockage occurred) are comparable to the reflectivity difference between the surface tilt and the adjacent tilt at 2.5° elevation angle. Consequently, no clear conclusion can be reached on the extent of beam blockage.

The second factor possibly contributing to the missed detection might be the shallowness of the event. The radar estimates the mean velocity over the vertical extent of the beam. If the outflow depth is low (e.g., < 200 m) and the velocities above the outflow flowing in the opposite direction (often the case), then the mean velocity estimate might well be less than the surface wind. This bias effect would be exacerbated if the event's outflow was partially shielded from the radar due to its location being in a valley and if the lower portion of the beam were blocked as discussed above.

## V. CONCLUSIONS

There were 42 microbursts that occurred over the Memphis mesonet for which radar and mesonet data were available. Of these, 40 were detected by both radar and mesonet, while the remaining 2 cases were detected by only the mesonet.

The first of two missed detection cases, 23-24 April 1985, did show, according to the actual winds encountered by the mesonet, a microburst signature which was accompanied by divergence and $\Delta V$'s which exceeded the threshold values used with the detection algorithm. This data used alone would suggest that a microburst was evident. The proximity of the event (as determined by the mesonet) to the radar appears to be a primary reason for not identifying it, while the apparent asymmetry of the microburst may be another contributing factor. These ideas seemed to be supported by the running of the microburst algorithm. It was shown that a shear region was detected but that a microburst event was not identified.

The case of 23 July 1985, according to the mesonet data, should be classified as a microburst event. However, the radar data did not portray a microburst signature. The Doppler velocity display showed only weak divergence and weak differential Doppler velocities. This qualitative assessment was verified by the microburst outflow detection algorithm whose output did not identify an event.

Two possible causes for why this event, which was located in a valley approximately 23 km west of the FL2 radar site, was undetected by the radar were addressed. The first of these factors identified was the problem of blockage to the radar beam. From analysis of the available radar data, blockage to the beam was not apparent. However, the radar data for this case did not include an appropriate sequence of tilts which would have aided in a more complete analysis. Therefore, it cannot be concluded with certainty that blockage to the beam was not a contributing cause to the missed detection. The second factor addressed could be attributed to the shallowness of the depth of the microburst outflow. It was noted that the outflow's mean velocity estimate might be less than the surface wind if:

(1) the outflow depth is low (e.g., <200 m), and

(2) the velocities above the outflow are flowing in the opposite direction.

It can be reasoned that both of these causes, along with the fact that the event was located in a valley, could have contributed to the missed detection of this microburst by the FL2 radar.

## VI. FUTURE WORK

Currently, there are plans to further compare the radar and mesonet wind fields. The wind histories as well as the wind magnitudes versus time will be analyzed for select cases. This analysis should help in the understanding of the headwind/tailwind estimation for microbursts. Also, the time delay (lag) that occurs between the time that the microburst is observed aloft by radar and the time at which it impacts the surface will be investigated.

## REFERENCES


Evans, J.E., and D. Johnson, 1984: The FAA Transportable Doppler Weather Radar. Preprints, 22nd Conference on Radar Meteorology. Zurich, Switzerland, American Meteorological Society, pp. 246-250.

Evans, J.E., and D. Turnbull, 1985: The FAA/MIT Lincoln Laboratory Doppler Weather Radar Program. Preprints, 2nd International Conference on the Aviation Weather System. Montreal, Canada, American Meteorological Society, pp. 76-79.

Fujita, T.T., 1985: The Downburst, Microburst and Macroburst. University of Chicago, 122 pp.

Merritt, M.W., 1987: Microburst Divergent Outflow Algorithm, Version 2. MIT Lincoln Laboratory Weather Radar Project Memorandum No. 43PM-WX-0004.

Rinehart, R.E., J.T. DiStefano, and M.M. Wolfson, 1986: Preliminary Memphis FAA Lincoln Laboratory Operational Weather Studies Results. MIT, Lincoln Laboratory Project Report ATC-141.

Wolfson, M.M., J.T. DiStefano, and B.E. Forman, 1986: The FLOWS Automatic Weather Station Network in Operation. MIT, Lincoln Laboratory Project Report ATC-134, FAA Report DOT-FAA-PM-85/27, 284 pp.

# REPORT DOCUMENTATION PAGE

| | |
|---|---|
| 1a. REPORT SECURITY CLASSIFICATION<br>Unclassified | 1b. RESTRICTIVE MARKINGS |
| 2a. SECURITY CLASSIFICATION AUTHORITY | 3. DISTRIBUTION/AVAILABILITY OF REPORT<br>Document is available to the public through the National Technical Information Service, Springfield, VA 22161. |
| 2b. DECLASSIFICATION/DOWNGRADING SCHEDULE | |
| 4. PERFORMING ORGANIZATION REPORT NUMBER(S)<br>ATC-142 | 5. MONITORING ORGANIZATION REPORT NUMBER(S)<br>DOT/FAA/PM-87/18 |
| 6a. NAME OF PERFORMING ORGANIZATION<br>Lincoln Laboratory, MIT<br>6b. OFFICE SYMBOL *(If applicable)* | 7a. NAME OF MONITORING ORGANIZATION<br>Electronic Systems Division |
| 6c. ADDRESS *(City, State, and Zip Code)*<br>P.O. Box 73<br>Lexington, MA 02173-0073 | 7b. ADDRESS *(City, State, and Zip Code)*<br>Hanscom AFB, MA 01731 |
| 8a. NAME OF FUNDING/SPONSORING ORGANIZATION<br>Department of Transportation<br>Federal Aviation Administration<br>Systems Research and Development Service<br>8b. OFFICE SYMBOL *(If applicable)* | 9. PROCUREMENT INSTRUMENT IDENTIFICATION NUMBER<br>F19628-85-C-0002 |
| 8c. ADDRESS *(City, State, and Zip Code)*<br>Washington, DC 20591 | 10. SOURCE OF FUNDING NUMBERS<br>PROGRAM ELEMENT NO. / PROJECT NO. 471 / TASK NO. / WORK UNIT ACCESSION NO. |

11. TITLE *(Include Security Classification)*

Study of Microburst Detection Performance During 1985 in Memphis, TN

12. PERSONAL AUTHOR(S)

John T. DiStefano

| 13a. TYPE OF REPORT | 13b. TIME COVERED | 14. DATE OF REPORT *(Year, Month, Day)* | 15. PAGE COUNT |
|---|---|---|---|
| Project Report | FROM _____ TO _____ | 1987, August 5 | 40 |

16. SUPPLEMENTARY NOTATION

None

| 17. COSATI CODES | | |
|---|---|---|
| FIELD | GROUP | SUB-GROUP |
| | | |
| | | |

18. SUBJECT TERMS *(Continue on reverse if necessary and identify by block number)*

low-level wind shear, microburst, Doppler weather radar, surface anemometers, mesonet, microburst outflow detection algorithm, radar/mesonet comparison, missed detections

19. ABSTRACT *(Continue on reverse if necessary and identify by block number)*

This report focuses on the detectability of microbursts using pulse Doppler weather radars and surface anemometers. The data used for this study were collected in the Memphis, TN area during the FLOWS* project of 1985. The methods used for declaring a microburst from both Doppler radar and surface anemometer data are described.

The main objective of this report was to identify the results that were generated by comparing the 1985 radar detected microbursts (which impacted the surface anemometer system) with the surface mesonet detected microbursts. In so doing, the issue of missed microburst detections, for which there occurred two (both by the radar), is identified. Possible reasons as to why these two microbursts were not detected are discussed in detail.

*FAA/Lincoln Laboratory Observational Weather Studies

| | |
|---|---|
| 20. DISTRIBUTION/AVAILABILITY OF ABSTRACT<br>☐ UNCLASSIFIED/UNLIMITED ☒ SAME AS RPT. ☐ DTIC USERS | 21. ABSTRACT SECURITY CLASSIFICATION<br>Unclassified |
| 22a. NAME OF RESPONSIBLE INDIVIDUAL<br>Maj. Thomas J. Alpert, USAF | 22b. TELEPHONE *(Include Area Code)*<br>(617) 863-5500, x-2330<br>22c. OFFICE SYMBOL<br>ESD/TML |